J Mater Sci (2007) 42:8120–8125
DOI 10.1007/s10853-007-1677-8

A new approach for estimation of Poisson's ratio of porous powder compacts

Kalyan Kumar Phani · Dipayan Sanyal

Received: 22 August 2006 / Accepted: 9 March 2007 / Published online: 12 June 2007

Abstract A new correlation between Poisson's ratio (v) and ultrasonic longitudinal wave velocity (V_L) has been established and the resulting correlation has been shown to agree well with experimental data on v versus V_L for a variety of porous powder compacts. Further, it has been demonstrated that ultrasonic longitudinal wave velocity can be used to estimate the elastic properties of sintered powder compacts.

Introduction

The elastic behaviour of sintered ceramic and metallic powder compacts are assuming great importance due to many novel usage of these materials with engineered pore structures, such as, cellular ceramics, metallic and ceramic foams and so on. Among the elastic properties, considerable research has been carried out for estimation of the effective Young's modulus (E) and shear modulus (G) of a porous body within a limited range of average porosity (p). Many theoretical correlations have been proposed for describing the variation of E and G with p [1–6]. In comparison, very little work has been done on the estimation of the effective Poisson's ratio (v) of a porous material, which, for structural calculations, is no less important than the other moduli E and G. Apart from its usefulness from the structural design point of view, Poisson's ratio is also unique among the elastic moduli in revealing information about interatomic forces. This property of v has been exploited to reveal the change in interatomic forces near the critical transition temperature T_C for high T_C superconductors [7]. However, the limited amount of research on the estimation of Poisson's ratio for porous materials has contributed to a debate regarding the porosity dependence of Poisson's ratio. While some argue that v is invariant with p [8], some others show the dependence of v on p [4, 9, 10]. Such debates may possibly be attributed to the fact that the Poisson's ratio is not directly measured, but derived from the Young's modulus and the bulk or shear modulus. The errors in measuring these moduli combine to yield values of v which are prone to inaccuracies of higher order. As a consequence, correlation of v versus p do not always fit experimental data very well as reported by Dean [3] and Arnold et al. [10]. In a recent study Phani and Sanyal [11] have reported an improved v versus p correlation which accounts also for the pore shape and established its efficacy with data for ribbon like pores [12] and spherical pores [13]. However, such correlations may have limited practical usage due to measurement difficulties of the ultrasonic shear wave velocity as discussed in the following paragraph.

Ultrasonic pulse-echo technique is a well-accepted method for determination of the elastic properties of dense and porous materials. For determination of v, it is necessary to measure two ultrasonic velocities, namely, the longitudinal wave velocity (V_L) and the shear wave velocity (V_S), respectively. Though V_L can be conveniently measured for a porous material, measurement of V_S creates appreciable difficulties as the transduction of shear wave through the material requires a good contact between the probe and the porous substrate. In some materials, such as, porous irradiated nuclear fuel material (e.g., UO_2), measurement of V_S through ultrasonic means is nearly impossible due to the

K. K. Phani (✉) · D. Sanyal
Central Glass and Ceramic Research Institute, 196 Raja S. C. Mullick Road, Kolkata 700032, India
e-mail: kkphani@cgcri.res.in

extreme fragility of the porous substrate [14] In such cases, an indirect measurement of V_S through the Rayleigh wave velocity V_R is done using acoustic microscopy [14]. From physical acoustic theory, one can write [15]:

$$\frac{E}{E_0} = \frac{\rho}{\rho_0}\left[\frac{(1+v)(1-2v)}{1-v}\right]\left[\frac{(1-v_0)}{(1+v_0)(1-2v_0)}\right]V_L^{*^2} \quad (1)$$

$$\frac{G}{G_0} = \frac{\rho}{\rho_0}\left[\frac{(1-2v)}{1-v}\right]\left[\frac{(1-v_0)}{(1-2v_0)}\right]V_L^{*^2} \quad (2)$$

where subscript 0 refers to the respective values of variables for pore free materials or mean polycrystalline (VRH) values calculated from single crystal data and normalized longitudinal velocity $V_L^* = V_L/V_{L0}$. These equations show that if the elastic properties of pore-free material are known, one can determine the elastic moduli only from the longitudinal velocity, V_L, provided the variation of v with the normalised longitudinal velocity is known.

The present study addresses the twin issues of exploring the feasibility of estimating effective Poisson's ratio with the help of ultrasonic longitudinal wave velocity V_L alone and developing an appropriate correlation which represents the variation of Poisson's ratio with porosity for a sintered powder compact.

Figure 1 shows the variation of the effective Poisson's ratio (v) with a function $f(v) = \frac{v_0}{1-v_0}V_L^*$which is a product of the normalised longitudinal velocity V_L^* and the parameter, $\frac{v_0}{1-v_0}$ calculated from Poisson's ratio of the pore free material. The significance of the above factor will be clarified in the subsequent section. Figure 1 clearly depicts that not only the effective Poisson's ratio is a function of $f(v)$ for a wide variety of powder compact materials (covering more than 200 data points) but also appear to fall on a single curve which is shown in the same figure. The derivation of the equation of the curve will be done in the subsequent section. A closer look at Fig. 1 reveals that at high longitudinal ultrasonic velocities (or low porosities) the experimental Poisson's ratio data closely follow the theoretical curve derived in this work, while at low velocities (or high porosities) the scatter of data around the suggested curve is more. Considering the fact that v is a derived property based on the ratio of E to G and at high porosities (low values of V_L^*) where E and G are both small, v is more prone to errors than at low porosities (high values of V_L^*), the scatter can be considered within acceptable limits. In the subsequent section, we systematically present our correlation of v versus V_L followed by another correlation of v versus p derived on the basis of V_L versus p of correlations developed earlier by Phani et al. [16, 17].

Analytical derivation

Equation (2) which expresses the effective shear modulus (G) as a function of effective Poisson's ratio v and the normalised longitudinal ultrasonic wave velocity V_L^* can yield a correlation between G and V_L^* only, provided a functional relationship between v and V_L^* can be established. This is possible because, for most porous materials, ρ/ρ_0 can be determined as a function of V_L^* from experimental data. Our first task was, therefore, to seek a correlation between $(1 - 2v)/(1 - v)$ versus V_L^*. Figure 2 shows the variation of $\Lambda(v) = (1 - 2v)/(1 - v)$ versus V_L^* for a

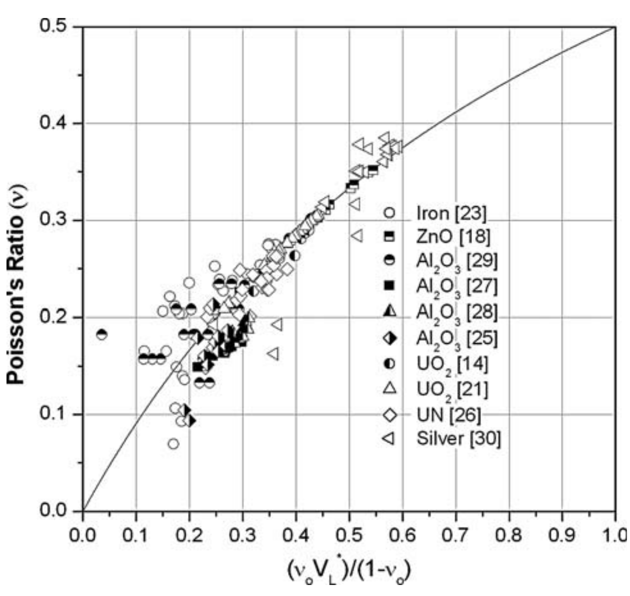

Fig. 1 Variation of the effective Poisson's ratio with $f(v)$

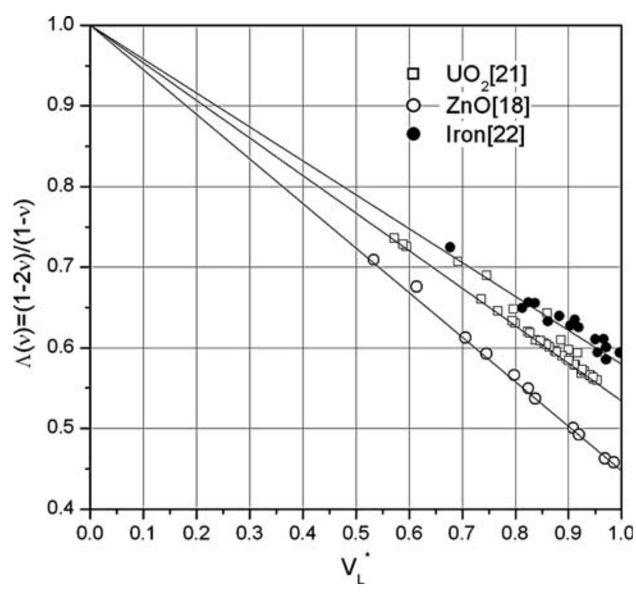

Fig. 2 Variation of the Poisson's ratio factor $\Lambda(v) = \frac{1-2v}{1-v}$ with V_L^*

number of oxides. In all cases, Λ (ν) decreases linearly with respect to the normalised velocity, V_L^*. Therefore, we assume that this variation can be described by the linear relation

$$\Lambda(\nu) = \Lambda_0 - \Lambda_1 \cdot V_L^* \tag{3}$$

where Λ (ν) = (1 – 2ν)/(1 – ν) and Λ_0 and Λ_1 are two constants. To make this equation compatible with the physical phenomena it represents, we determine the value of the constants from the boundary conditions

$$\begin{array}{lll} \text{at} & V_L^* = 0 & \nu = 0 \\ \text{at} & V_L^* = 1 & \nu = \nu_o \end{array}$$

Substituting these values in Eq. 3 yields Λ_0 = 1 and $\Lambda_1 = \frac{\nu_0}{1-\nu_0}$. Equation 3 can now be written in terms of a Λ_0 and Λ_1 as

$$\Lambda(\nu) = 1 - \frac{\nu_0}{1-\nu_0} V_L^* \tag{4}$$

For all the oxides shown in Fig. 2, Eq. 4 has been plotted using the ν_o values of 0.356, 0.318 and 0.296 for ZnO, UO_2 and iron, respectively. These values were taken from single crystal data reported in the literature [18–20]. Considering the scatter in the ν values as discussed earlier, the agreement between Eq. 4 and the data can be considered as extremely good. From Eq. 4, it is evident that the Poisson's ratio ν is a function of V_L^*, which is given by the following relation:

$$\nu = \frac{\frac{\nu_0}{1-\nu_0} V_L^*}{1 + \frac{\nu_0}{1-\nu_0} V_L^*} \tag{5}$$

The parameter $\frac{\nu_0}{1-\nu_0} V_L^*$ is nothing but the non-dimensional function $f(\nu)$ in the abscissa of Fig. 1. This factor has been chosen to draw Fig. 1 to facilitate the representation of all the data for oxides in a single curve of the rectangular hyperbola which is given by Eq. 5.

Because of the scatter in the data, the agreement between the data and the equation can only be judged qualitatively. However, an indirect way of verifying the accuracy of the proposed correlation is to assume that Eq. 5 is exact and predict the other elastic properties such as shear are bulk moduli based on this equation and compare them with the corresponding experimental data.

Considering Eqs. 2 and 4, one can write:

$$\frac{G}{G_0} = \frac{\rho}{\rho_0}\left[1 - \Lambda_1 V_L^*\right] m V_L^{*^2} \tag{6}$$

where m = (1 – ν_0)/(1 – 2ν_0), which is a constant for a specific material.

To express the above relation in terms of V_L^* alone, ρ/ρ_0 must be expressed in terms of V_L^*. The dependence of the ultrasonic velocity on porosity can best be described by a power law relation of the form [17, 18]:

$$V_L^* = (1-p)^n \tag{7}$$

where the exponent n is dependent on the pore morphology of the material [17]. In the lower porosity limit, a series expansion of Eq. 7 reduces to the linear relation when higher order terms in p are neglected:

$$V_L^* = 1 - np \tag{8}$$

where the porosity is expressed in terms of the relative density as

$$p = 1 - \rho/\rho_0 \tag{9}$$

Combining Eqs. 8 and 9, we get:

$$\frac{\rho}{\rho_0} = \frac{V_L^* + n - 1}{n} \tag{10}$$

Finally a relation between the shear modulus, G and the longitudinal ultrasonic velocity, V_L^* is obtained by combining Eqs. 6 and 10, as follows:

$$G^* = \frac{m\left(V_L^* + n - 1\right)\left(1 - \Lambda_1 V_L^*\right)}{n} V_L^{*^2} \tag{11}$$

Equation 11 shows that the shear modulus can be calculated from longitudinal ultrasonic velocity, V_L only knowing the value of n and the pore free material properties.

A similar equation can also be derived for bulk modulus:

$$\frac{K}{K_o} = K^* = \frac{m_1\left(V_L^* + n - 1\right)\left(1 + 2\Lambda_1 V_L^*\right)}{n} V_L^{*^2} \tag{12}$$

where K^* is the normalized bulk modulus and $m_1 = \frac{1-\nu_0}{1+\nu_0}$.

Results and discussion

Figure 3 is a plot of ultrasonic longitudinal wave velocity versus porosity for uranium dioxide reported by various researchers [14, 15, 21]. The Eq. 8 was fitted to the data taking V_{L0} value of 5478.96 m/s (calculated from mean polycrystalline (VRH) values obtained from measured single crystal data of UO_2 [20]) giving a value of n = 1.701. The fit between the data and the equation was evaluated in terms of the sum of squares, Q, given by:

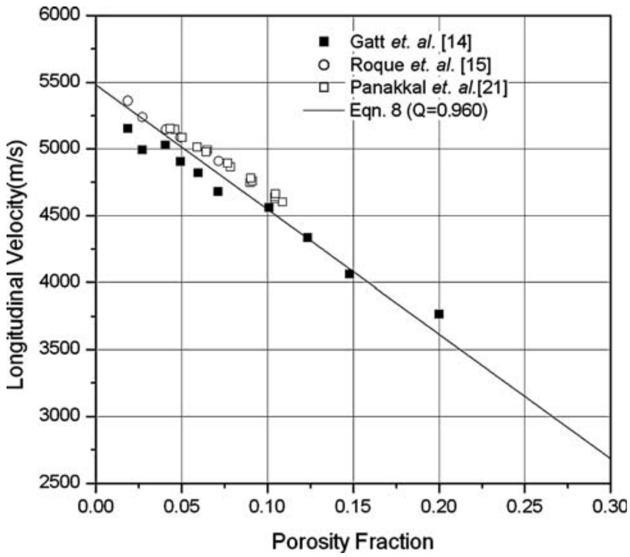

Fig. 3 Variation of the ultrasonic longitudinal wave velocity of UO_2 with porosity

$$Q = 1 - \frac{\sum_{i=1}^{n} (S_i - \hat{S}_i)^2}{\sum_{i=1}^{n} (S_i - \bar{S})^2} \qquad (13)$$

where $\bar{S}$ and $\hat{S}_i$ are the mean and the theoretically estimated modulus values, respectively. A value of $Q = 0.960$ indicates a good fit between the two.

Figure 4 is a plot of normalized shear modulus (G^*) versus normalized longitudinal velocity (V_L^*) for uranium dioxide data reported by Gatt et al. [14] and Boocock et al. [21]. G^* values are calculated using the pore free material value of G_0 = 87.4 GPa. Also shown on the plot Eq. 11 with n = 1.701. The plot shows an excellent agreement between the experimental data with the values predicted from Eq 11. Both the datasets exhibit a very good fit with a very high value of Q which is given in Fig. 4. The maximum deviation of G value predicted from Eq. 11 is within ±6% of the experimental one. A more sensitive test for the validation of the correlation for Poisson's ratio given by Eq. 5 is a comparison between the normalised bulk modulus (K^*) calculated from the measured values of E^* and G^* with the values predicted from Eq. 12. Figure 5 shows K^* values for UO_2, estimated from the corresponding values of E^* and G^* plotted against normalized velocity (V_L^*) for the data reported by Gatt et al. [14] and Boocock et al. [21] along with the plot of Eq. 12. The agreement between the data reported by Gatt et al. [14] and Eq. 12 is excellent having a value of Q = 0.996. For Boocock et al.'s data, the closeness of the calculated points to the theoretical curve is acceptable (Q = 0.868) considering the sensitivity of these calculations to the propagation of experimental errors in measurement of E and G.

For the other two powder compacts namely ZnO and iron reported by Martin et al. [18], Panakkal et al. [22], Spitzig et al. [20], Yeheskel [23] and Beiss et al. [24], predicted G values from Eq. 11 also showed excellent agreement with the experimental data having Q values varying in the range of 0.970–0.981. However, only the comparison of bulk modulus is given here. For this purpose, the bulk modulus (K) for ZnO and iron powder compacts were estimated from E and G. The values were normalized using pore free material bulk moduli values of

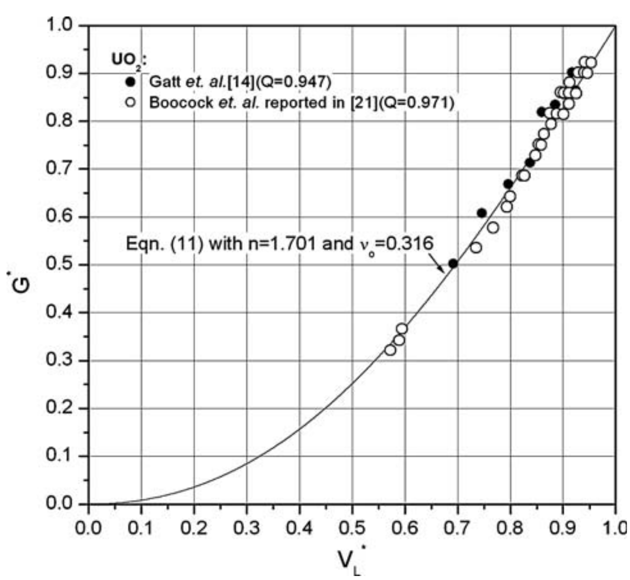

Fig. 4 Variation of the normalised shear modulus of UO_2 with normalised ultrasonic longitudinal velocity

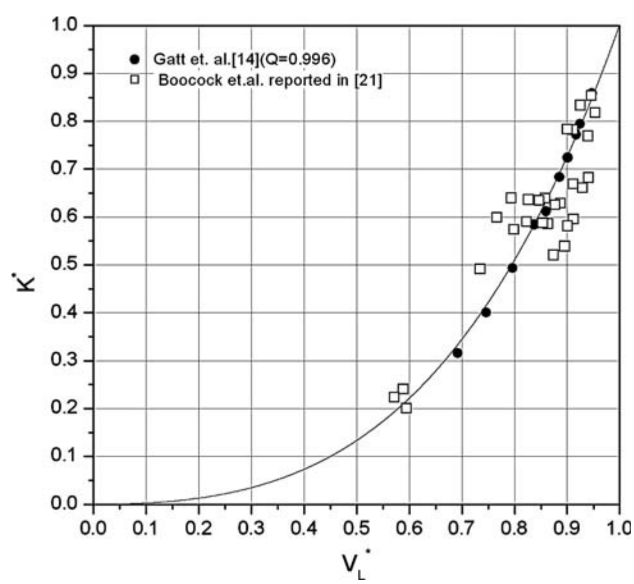

Fig. 5 Variation of the normalised bulk modulus of UO_2 with normalised ultrasonic longitudinal velocity

143.6 and 168.7 GPa and longitudinal velocity values of 5972.9 and 5960.0 m/s for ZnO and iron, respectively. The values *n* were estimated as 1.510 and 1.923 from Eq. 8 for ZnO and iron, respectively from the experimental data [18, 22]. Figure 6 shows the plot of K^* versus V_L^* for ZnO and iron powder compacts along with the plots of Eq. 12. In both cases, the predicted values show excellent agreement with the data having *Q* values of 0.996 and 0.986 for ZnO and iron, respectively. Thus, it is established that the proposed correlation between the Poisson's ratio and the normalised velocity given by Eq. 5 holds well for a range of oxide ceramics and powder compacts.

Equation 8 can be combined with Eqs. 5, 11 or 12 to predict variation of *v*, *G* or *K* with porosity. For *v* the equation is given by

$$v = \frac{A_1(1 - np)}{1 + A_1(1 - np)} \quad (14)$$

Equation 14 along with Poisson's ratio versus porosity data reported by Panakkal [21] has been plotted in Fig. 7. Considering the scatter in *v* values for reasons mentioned earlier, the agreement between Eq. 14 and data can be considered acceptable even though the *Q* value is 0.78 and it predicts correctly the trend in the reduction of *v* with porosity.

Conclusion

A new correlation between Poisson's ratio and longitudinal ultrasonic velocity has been suggested and shown to agree extremely well with experimental data for a number of powder compacts. The elastic property values of materials prepared from powder compacts predicted based on this equation using physical acoustics theory agree with the experimental data within ±6%. Considering the error involved in experimental determination of these elastic moduli, we regard the fit to be quite good for the purpose of quantitative non-destructive evaluation of the Poisson's ratio and other elastic moduli.

Moreover, it is established that ultrasonic longitudinal wave velocity alone can be used for the determination of elastic properties of materials. Variation of Poisson's ratio with porosity predicted from the proposed equation also agrees quite well with the experimental data.

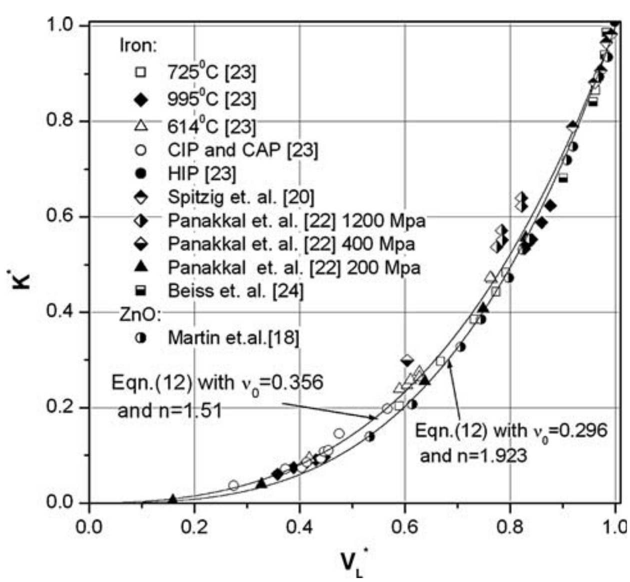

Fig. 6 Variation of the normalised bulk modulus of ZnO and Iron with normalised ultrasonic longitudinal velocity

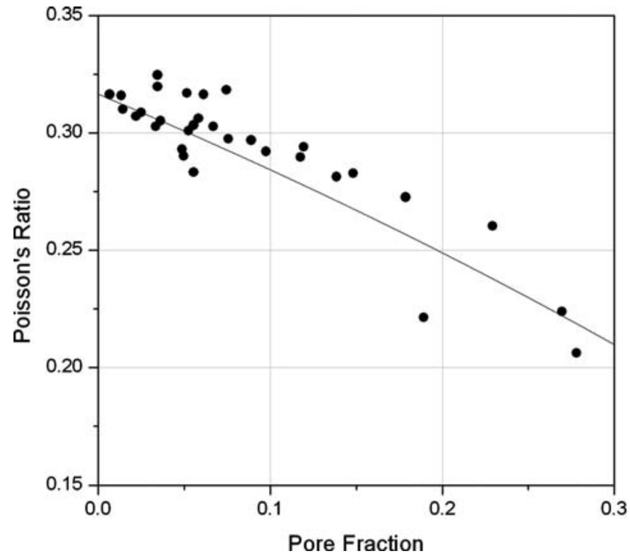

Fig. 7 Variation of Poisson's ratio of UO_2 with porosity

Acknowledgements The authors are thankful to the Director, CG&CRI for his permission to publish this work.

References

1. Hashin Z, Shtrikman S (1961) J Franklin Inst 271:3361
2. Dean EA (1983) J Amer Ceram Soc 66:847
3. Nielsen LF (1984) J Amer Ceram Soc 67:93
4. Zimmerman RW (1992) Mech Res Comm 19:563
5. Phani KK (1996) J Mater Sci 31:272
6. Rice RW (1998) Porosity in ceramics. Marcel Dekker Inc, New York
7. Dunn ML, Ledbetter H (1995) J Mater Res 10:2715
8. Wang JC (1984) J Mater Sci 19:801
9. Ramakrishna N, Arunachalam VS (1990) J Mater Sci 25:3930
10. Arnold M, Boccaccini AR, Ondracek G (1996) J Mater Sci 31:1643
11. Phani KK, Sanyal D (2005) J Mater Sci 40:5685
12. Ashkin D, Haber RA, Wachtman JB (1990) J Am Ceram Soc 73:3376
13. Walsh JB, Brace WF, England AW (1965) J Am Ceram Soc 48:605

14. Gatt J-M, Monerie Y, Laux D, Baron D (2005) J Nuclear Mater 336:145
15. Roque V, Cros B, Baron D, Dehaudt P (2000) J Nuclear Mater 277:211
16. Phani KK, Niyogi SK (1986) J Mater Sci Lett 5:427
17. Maitra AK, Phani KK (1994) J Mater Sci 29:4415
18. Martin LP, Dadon D, Rosen M (1996) J Am Ceram Soc 79:1281
19. Wachtman JB,Wheat ML,Anderson HJ, Bates JL (1965) J Nuclear Mater 16:39
20. Spitzig WA, Thompson RB, Jules DC (1989) Metal Trans 20A:571
21. Panakkal JP (1991) IEEE Trans Ferroelec Freq Control 38:161
22. Panakkal JP, Willems H, Arnold W (1990) J Mater Sci 25:1397
23. Yeheskel O (2004) J Testing Eval 32:17
24. Beiss P, Sander C (1998) in Proceedings of the International Congress on Powder Technology, Granada, Spain, 2:552
25. Nagarajan A (1971) J App Physics 42:3693
26. Padel A, Novion CD (1969) J Nucl Mater 33:40
27. Asmani M, Kermel C, Leriche A, Ourak M (2001) J Euro Ceram Soc 21:1081
28. Chang LS, Chuang TH, Wei WJ (2000) Mater Character 45:221
29. Green DJ, Nader C, Brezny R (1990) Ceram Trans 7:345
30. Yeheskel O, Shokhat M, Ratzker M, Dariel MP (2001) J Mater Sci 36:1219